Electronic Supplementary Material (ESI) for Organic & Biomolecular Chemistry


# In-Peptide Synthesis of Di-Oxazolidinone and Dehydroamino Acid-Oxazolidinone Motives as β-Turns Inducers *Supporting Information*

Rossella De Marco, Arianna Greco, Sebastiano Rupiani, Alessandra Tolomelli, Claudia Tomasini, Silvia Pieraccini, Luca Gentilucci*

*Dept. of Chemistry "G. Ciamician", University of Bologna, via Selmi 2, 40126 Bologna Italy*

** E-mail: luca.gentilucci@unibo.it; Phone: +39 0512099570; Fax: +39 0512099456*

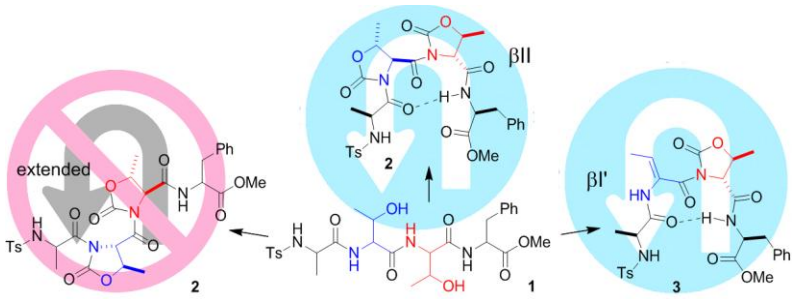


Constraining a peptide in a snap: linear peptides **1** give rise in a single step to sequences $Oxd^2$-$Oxd^3$ (**2**) or $\Delta Abu^2$-$Oxd^3$ (**3**); these scaffolds adopt well defined extended or folded conformations, in particular normal or inverse β-turns of type I or II.

***Table of contents***

$^1$H-NMR characterization of the model compounds **2a**,**c**,**d**, and **3b**,**c** at 400 MHz in 8:2 DMSO-$d_6$/$H_2O$.

Ts-Ala-(5'Me-Oxd$^2$)-(5'Me-Oxd$^3$)-PheOMe (**2a**). $^1$H-NMR δ: 1.18 (d, J=6.7 Hz, 3H, AlaMe), 1.44-1-47 (m, 6H, Oxd$^3$Me+Oxd$^2$Me), 2.37 (s, 3H, TsMe), 2.94 (dd, J=8.4, 13.9 Hz, 1H, PheHβ), 3.01 (dd, J=5.7, 13.9 Hz, 1H, PheHβ), 3.56 (s, 3H, OMe), 4.48-4.52 (m, 2H, PheHα+Oxd$^3$$H_5$), 4.57 (d, J=1.9 Hz, 1H, Oxd$^3$$H_4$), 4.66 (dq, J=2.0, 7.0 Hz, 1H, Oxd$^2$$H_5$), 5.02 (dq, J=6.7, 8.5 Hz, 1H, AlaHα), 5.17 (d, J=2.0 Hz, 1H, Oxd$^2$$H_4$), 7.11 (d, J=7.6 Hz, 2H, PheArH), 7.14-7.26 (m, 3H, PheArH) 7.37 (d, J=8.0 Hz, 2H, TsArH), 7.63 (d, J=8.0 Hz, 2H, TsArH), 8.36 (d, J=8.5 Hz, 1H, AlaNH), 8.98 (d, J=7.0 Hz, 1H, PheNH).

Ts-Ala-ΔAbu-(5'Me-Oxd)-PheOMe (**3b**). $^1$H-NMR δ: 1.03 (d, J=7.2 Hz, 3H, AlaMe), 1.36 (d, J=6.2 Hz, 3H, OxdMe), 1.66 (d, J=7.2 Hz, 3H, ΔAbuMe), 2.40 (s, 3H, TsMe), 2.98 (dd, J=7.2, 14.0 Hz, 1H, PheHβ), 3.04 (dd, J=6.0, 14.0 Hz, 1H, PheHβ), 3.59 (s, 3H, OMe), 3.90 (quint, J=6.4 Hz, 1H, AlaHα), 4.33 (dq, J=2.8, 6.2 Hz, 1H, Oxd$H_5$), 4.42 (d, J=2.8 Hz, 1H, Oxd$H_4$), 4.54 (q, J=7.4 Hz, 1H, PheHα), 5.71 (q, J=7.2 Hz, 1H, ΔAbuHβ), 7.18-7.25 (m, 3H, PheArH), 7.31 (t, J=7.4 Hz, 2H, PheArH), 7.38 (d, J=8.1 Hz, 2H, TsArH), 7.68 (d, J=8.1 Hz, 2H, TsArH), 7.94 (d, J=7.6 Hz, 1H, AlaNH), 8.78 (d, J=7.2 Hz, 1H, PheNH), 9.53 (s, 1H, ΔAbuNH).

Ts-Ala-(5'Me-Oxd$^2$)-D-(5'Me-Oxd$^3$)-Phe-OMe (**2c**). $^1$H-NMR δ: 1.17 (d, J=6.8 Hz, 3H, AlaMe), 1.35 (d, J=6.2 Hz, 3H, Oxd$^2$Me), 1.39 (d, J=6.4 Hz, 3H, Oxd$^3$Me), 2.36 (s, 3H, TsMe), 2.83 (dd, J=8.1, 13.8 Hz, 1H, PheHβ), 3.11 (dd, J=8.1, 13.8 Hz, 1H, PheHβ), 3.63 (s, 3H, OMe), 3.84 (quint, J=5.6 Hz, 1H, Oxd$^3$$H_5$), 4.36 (d, J=4.8 Hz, 1H, Oxd$^3$$H_4$), 4.51 (dq, J=8.1, 9.6 Hz, 1H, PheHα), 4.95-5.03 (m, 2H, Oxd$^2$$H_4$+AlaHα), 5.06 (q, 1H, J=6.2 Hz, Oxd$^2$$H_5$), 7.17 (d, J=6.8 Hz, 2H, PheArH), 7.19-7.30 (m, 3H, PheArH), 7.37 (d, J=8.2 Hz, 2H, TsArH), 7.62 (d, J=8.2 Hz, 2H, TsArH), 8.42 (d, J=9.2 Hz, 1H, AlaNH), 8.94 (d, J=8.1 Hz, 1H, PheNH).

Ts-Ala-ΔAbu-D-(5'MeOxd)-PheOMe (**3c**). $^1$H-NMR δ: 1.03 (d, J=7.2 Hz, 3H, AlaMe), 1.20 (d, J=6.0 Hz, 3H, OxdMe), 1.67 (d, J=7.2 Hz, 3H, ΔAbuMe), 2.36 (s, 3H, TsMe), 2.85 (dd, J=10.4, 13.5 Hz, 1H, PheHβ), 3.12 (dd, J=4.8, 13.5 Hz, 1H, PheHβ), 3.58-3.69 (m, 4H, Oxd$H_5$+OMe), 3.99 (quint, J=7.1 Hz, 1H, AlaHα), 4.25 (d, J=2.0 Hz, 1H, Oxd$H_4$), 4.58 (m, 1H, PheHα), 5.65 (q, J=6.8 Hz, 1H, ΔAbuHβ), 7.13-7.24 (m, 2H, PheArH), 7.28 (t, J=7.0 Hz, 2H, PheArH), 7.35 (d, J=6.6 Hz, 2H, TsArH), 7.65 (d, J=6.6 Hz, 2H, TsArH), 7.93 (d, J=8.4 Hz, 1H, AlaNH), 8.85 (d, J=8.4 Hz, 1H, PheNH), 9.73 (s, 1H, ΔAbuNH).

Ts-Ala-(5'Me-Oxd$^2$)-D-(5'Me-Oxd$^3$)-D-PheOMe (**2d**). $^1$H-NMR δ: 1.15 (d, J=6.6 Hz, 3H, AlaMe), 1.40 (d, J=6.2 Hz, 3H, Oxd$^2$Me), 1.46 (d, J=6.0 Hz, 3H, Oxd$^3$Me), 2.37 (s, 3H, TsMe), 2.97 (d, J=6.8 Hz, 2H, PheHβ), 3.58 (s, 3H, OMe), 4.46-4.52 (m, 3H, PheHα+Oxd$^3$$H_{4,5}$), 5.02 (m, 1H, AlaHα), 5.03 (d, J=1.6 Hz, 1H, Oxd$^2$$H_4$), 5.10 (dq, J=1.6, 6.2 Hz, 1H, Oxd$^2$$H_5$), 7.18 (d, J=6.7 Hz, 2H, PheArH), 7.19-7.23 (m, 3H, PheArH), 7.37 (d, J=8.2 Hz, 2H, TsArH), 7.62 (d, J=8.2 Hz, 2H, TsArH), 8.41 (d, J=9.6 Hz, 1H, AlaNH), 8.89 (d, J=7.6 Hz, 1H, PheNH).

**TableS1**. Selected $^{1}$H-NMR chemical shifts (δ) of the model compds **2a**, **2c**, **2d**, and **3b**, **3c**, solvents: S1 = $CDCl_3$; S2 = 8:2 DMSO-$d_6$/$H_2O$; amino acid stereochemistry has been omitted.

| | **2a** | | **2c** | | **2d** | | **3b** | | **3c** | |
|---|---|---|---|---|---|---|---|---|---|---|
| | S1 | S2 | S1 | S2 | S1 | S2 | S1 | S2 | S1 | S2 |
| Ala$^{1}$NH | 5.39 | 8.36 | 5.44 | 8.42 | 5.61 | 8.41 | 5.92 | 7.94 | 5.66 | 7.93 |
| Ala$^{1}$Hα | 5.22 | 5.02 | 5.11 | 5.0 | 5.16 | 5.02 | 3.85 | 3.90 | 3.87 | 3.99 |
| Oxd$^{2}$H4 | 5.26 | 5.17 | 5.24 | 5.0 | 5.42 | 5.03 | - | - | - | - |
| Oxd$^{2}$H5 | 4.58 | 4.66 | 4.53 | 5.06 | 4.58 | 5.10 | - | - | - | - |
| ΔAbuNH | - | - | - | - | - | - | 8.66 | 9.53 | 8.28 | 9.73 |
| ΔAbuHβ | - | - | - | - | - | - | 6.04 | 5.71 | 6.27 | 5.65 |
| Oxd$^{3}$H4 | 4.26 | 4.57 | 4.29 | 4.36 | 4.3 | 4.5 | 4.38 | 4.42 | 4.4 | 4.25 |
| Oxd$^{3}$H5 | 4.75 | 4.5 | 4.64 | 3.84 | 4.3 | 4.5 | 4.4 | 4.33 | 4.6 | 3.6 |
| Phe$^{4}$NH | 6.28 | 8.98 | 6.55 | 8.94 | 6.63 | 8.89 | 7.64 | 8.78 | 7.98 | 8.85 |
| Phe$^{4}$Hα | 4.85 | 4.5 | 4.82 | 4.51 | 4.88 | 4.5 | 4.84 | 4.54 | 4.79 | 4.58 |

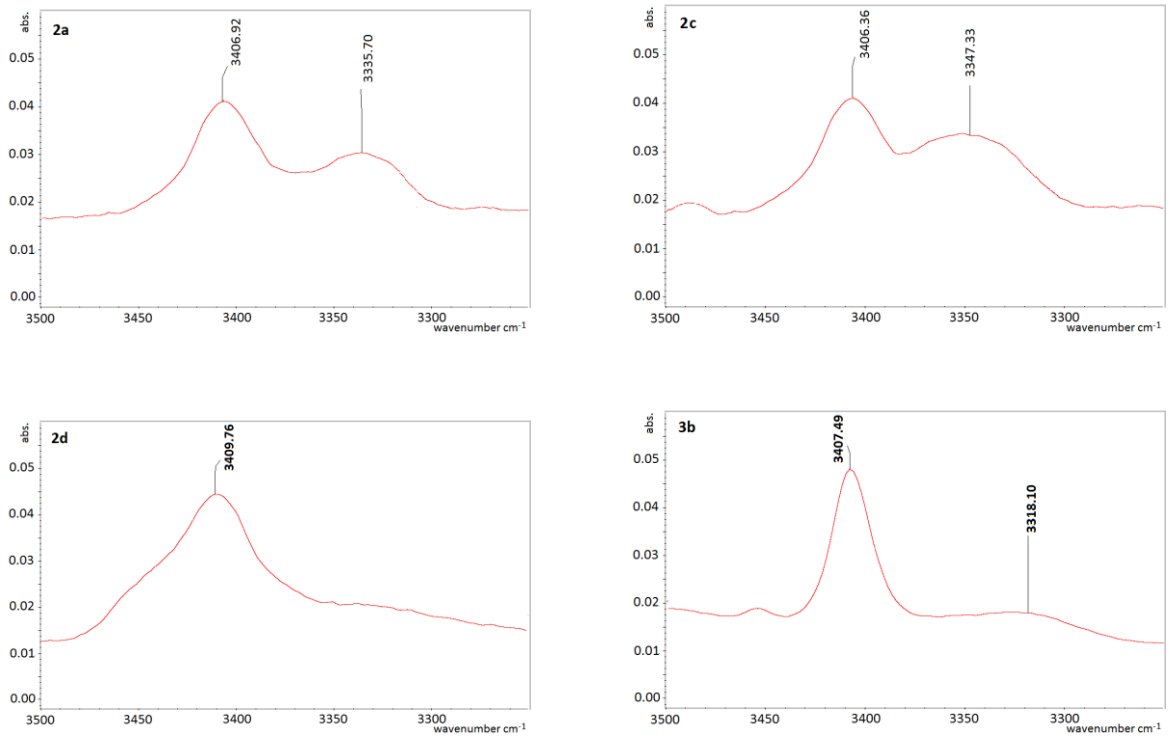


**Figure S1.** Amide NH stretching regions of the IR absorption spectra for samples of tetrapeptides **2a**, **2d** and **3b** (3 mM in DCM) at room temperature.

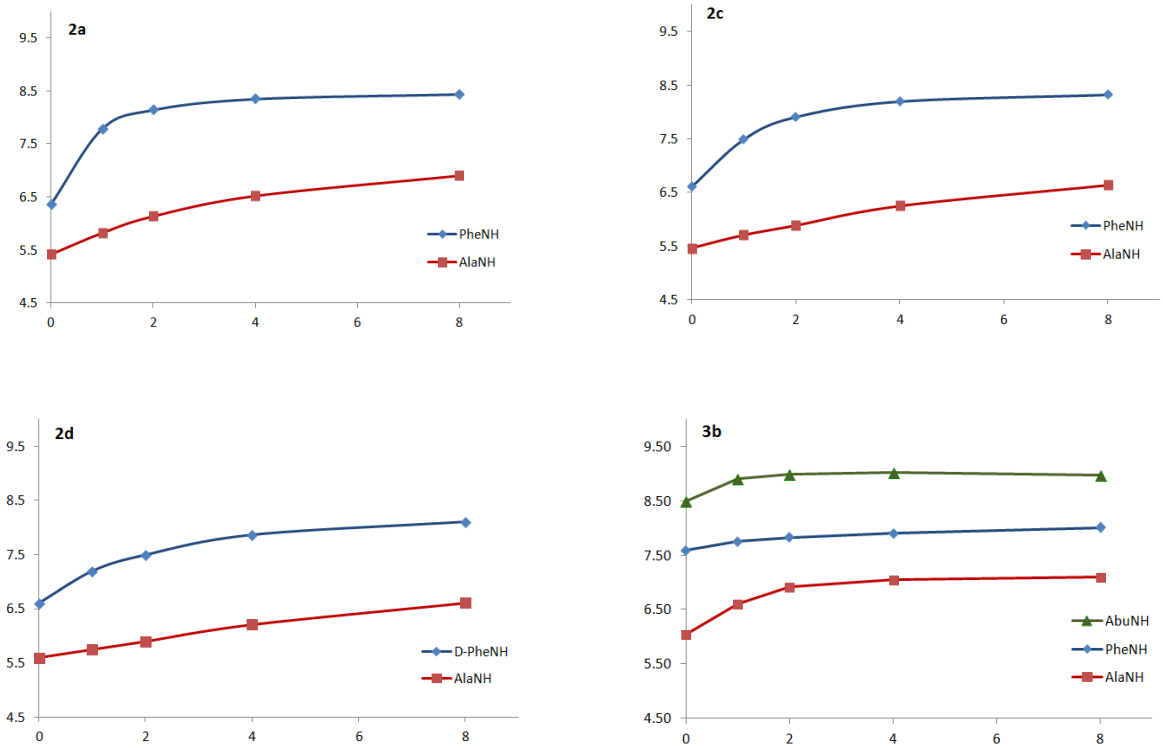


**Figure S2.** Variation of NH proton chemical shift (p.p.m.) of **2a**, **2c**, **2d** and **3b** as a function of increasing percentages of DMSO-$d_6$ to the $CDCl_3$ solution (v/v).

**Table S2.** Non-obvious ROESY cross-peaks observed for **2a**.[a]

| Cross-peak | intensity | Cross-peak | intensity |
|---|---|---|---|
| PheNH-Oxd$^3$Me | w | PheNH-PheHβ(up) | s |
| PheNH-PheHβ(dw) | m | PheNH-PheHα | m |
| PheNH-Oxd$^3$H4 | s | PheNH-Oxd$^3$H5 | m |
| PheNH-Oxd$^2$H5 | w | PheNH-PheArH | m |
| AlaNH-AlaMe | vs | AlaNH-AlaHα | s |
| AlaNH-TsArH2,6 | s | TsArH2,6-AlaMe | w |
| TsArH2,6-Oxd$^2$Me | w | TsArH2,6-AlaHα | m |
| TsArH3,5-Oxd$^2$Me | s | TsArH3,5- Oxd$^2$H4 | w |
| PheArH-PheHα | s | Oxd$^2$H4-Oxd$^3$H4 | w |
| Oxd$^2$H4-AlaHα | w | AlaHα-Oxd$^2$H5 | w |
| Oxd$^2$H5-Oxd$^3$H5 | w | COOMe-PheHα | w |

[a] Stereochemistry has been omitted; [b] up = upfield, dw = downfield; [c] vs = very strong, s = strong, m = medium, w = weak.

**Table S3.** Non-obvious ROESY cross-peaks observed for **2c**.[a]

| Cross-peak | intensity | Cross-peak | intensity |
|---|---|---|---|
| PheNH-PheArH | w | PheNH-PheHα | m |
| PheNH-Oxd$^3$H4 | vs | PheNH-Oxd$^3$H5 | w |
| PheNH-PheHβ(dw) | w | PheNH-PheHβ(up) | s |
| PheNH-Oxd$^3$Me | w | PheNH-COOMe | w |
| AlaNH-TsArH2,6 | m | AlaNH-AlaHα | m |
| AlaNH-AlaMe | s | TsArH2,6-AlaMe | w |
| TsArH2,6-Oxd$^2$Me | w | TsArH2,6-AlaHα | m |
| TsArH3,5-Oxd$^2$Me | w | TsArH3,5-AlaHα | w |
| PheArH2,4,6- Oxd$^3$Me | w | PheArH2,4,6- PheHβ(up) | s |
| PheArH2,4,6- PheHβ(dw) | s | PheArH2,4,6- AlaMe | w |
| PheArH2,4,6- PheHα | m | PheArH2,4,6-COOMe | w |
| PheArH2,4,6-Oxd$^3$H5 | w | Oxd$^2$H4-Oxd$^3$H5 | w |
| Oxd$^2$H4-Oxd$^3$H4 | w | Oxd$^2$H5-Oxd$^3$H4 | w |
| Oxd$^2$H5-PheHα | w | AlaHα-PheHα | w |
| PheHα-PheHβ(dw) | s | PheHα-PheHβ(up) | m |
| PheHα-COOMe | w | PheHα- Oxd$^3$H5 | w |
| PheHα-Oxd$^3$H4 | w | Oxd$^3$H5-PheHβ(dw) | w |
| COOMe-AlaMe | m | COOMe-TsMe | w |
| COOMe-PheHβ(dw) | m | COOMe-PheHβ(up) | m |
| TsMe- Oxd$^2$Me | w | | |

[a] Stereochemistry has been omitted; [b] up = upfield, dw = downfield; [c] vs = very strong, s = strong, m = medium, w = weak.

**Table S4.** Non-obvious ROESY cross-peaks observed for **2d**.[a]

| Cross-peak | intensity | Cross-peak | intensity |
|---|---|---|---|
| PheNH-AlaMe | w | PheNH-Oxd$^3$Me | w |
| PheNH-PheHβ | vs | PheNH-COOMe | w |
| PheNH-PheHα | m | PheNH-Oxd$^3$H4 | m |
| PheNH-Oxd$^3$H5 | w | PheNH-PheArH | s |
| AlaNH-AlaMe | s | AlaNH-COOMe | w |
| AlaNH-AlaHα | s | AlaNH-TsArH2,6 | s |
| AlaNH-TsArH3,5 | w | TsArH2,6-AlaMe | m |
| TsArH2,6-Oxd$^2$Me | w | TsArH2,6-AlaHα | s |
| TsArH2,6-OxdH4 | w | TsArH3,5-Oxd$^2$Me | s |
| TsArH3,5-AlaHα | m | PheArH3,5-AlaMe | m |
| PheArH3,5-COOMe | w | PheArH3,5-PheHα | m |
| PheArH-Oxd$^3$Me | w | PheArH-COOMe | s |
| Oxd$^2$H4-TsMe | m | PheHα-AlaMe | w |
| COOMe-AlaMe | w | COOMe-PheHβ | s |
| PheHβ-AlaMe | m | TsMe-AlaMe | w |
| Oxd$^2$Me-AlaMe | w | | |

[a] Stereochemistry has been omitted; [b] up = upfield, dw = downfield; [c] vs = very strong, s = strong, m = medium, w = weak.

**Table S5.** Non-obvious ROESY cross-peaks observed for **3b.**[a]

| Cross-peak | intensity | Cross-peak | intensity |
|---|---|---|---|
| ΔAbuNH-AlaMe | m | ΔAbuNH-ΔAbuMe | s |
| ΔAbuNH-AlaHα | vs | ΔAbuNH-AlaNH | s |
| ΔAbuNH-PheNH | w | ΔAbuNH-TsArH2,6 | w |
| PheNH-Oxd$^3$H5 | w | PheNH-PheHβ | vs |
| PheNH-Oxd$^3$H4 | vs | PheNH-PheHα | s |
| PheNH-PheArH | m | PheNH-AlaNH | w |
| AlaNH-AlaMe | vs | AlaNH-AlaHα | s |
| AlaNH-TsArH2,6 | w | TsArH2,6-AlaMe | w |
| TsArH2,6-AlaHα | m | PheArH-COOMe | w |
| PheArH-PheHβ | vs | PheArH-PheHα | s |
| PheArH-Oxd$^3$H5 | w | ΔAbuHb-Oxd$^3$H4 | w |
| COOMe-PheHβ | m | COOMe-PheHα | w |
| PheHβ-Oxd$^3$H4 | w | COOMe-Oxd$^3$Me | w |
| ΔAbuMe-TsMe | w | ΔAbuMe-AlaMe | s |
| ΔAbuMe-Oxd$^3$Me | w | | |

[a] Stereochemistry has been omitted; [b] up = upfield, dw = downfield; [c] vs = very strong, s = strong, m = medium, w = weak.

**Table S6.** Non-obvious ROESY cross-peaks observed for **3c**.[a]

| Cross-peak | intensity | Cross-peak | intensity |
|---|---|---|---|
| ΔAbuNH-AlaMe | m | ΔAbuNH-ΔAbuMe | s |
| ΔAbuNH-Oxd$^3$Me | w | ΔAbuNH-AlaNH | vs |
| ΔAbuNH-ΔAbuHβ | w | ΔAbuNH-TsArH2,6 | w |
| ΔAbuNH-PheNH | w | PheNH-PheArH | m |
| PheNH-PheHβ(up) | s | PheNH-PheHβ(dw) | w |
| PheNH-Oxd$^3$H5 | m | PheNH-Oxd$^3$H4 | s |
| PheNH-PheHα | s | PheNH-PheArH | m |
| AlaNH-AlaMe | m | AlaNH-AlaHα | m |
| TsArH2,6-AlaMe | m | TsArH2,6-AlaHα | s |
| TsArH2,6-AlaNH | m | TsArH3,5-AlaNH | w |
| PheArH3,5-Oxd$^3$Me | w | PheArH3,5-PheHβ(up) | w |
| PheArH3,5-PheHα | w | PheArH2,6-Oxd$^3$Me | w |
| PheArH2,6-PheHβ(up) | vs | PheArH2,6-PheHβ(dw) | vs |
| PheArH2,6-Oxd$^3$H5 | w | PheArH2,6-PheHα | s |
| PheHα-PheHβ(dw) | vs | PheHα-PheHβ(up) | s |
| Oxd3H5-PheHβ(up) | w | COOMe-PheNH | w |
| COOMe-PheHα | m | COOMe-PheHβ(dw) | w |
| COOMe-PheHβ(up) | w | | |

[a] Stereochemistry has been omitted; [b] up = upfield, dw = downfield; [c] vs = very strong, s = strong, m = medium, w = weak.

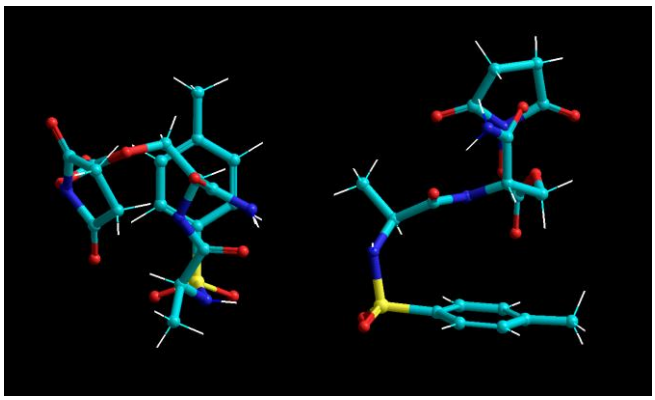

**Figure S3.** Top (left) and side (right) view of the intermediate anion **A** of Scheme 1, calculated for the cyclization of the model peptide Ts-Ala-Ser-$NH_2$ with DSC and DIPEA, employing ab initio molecular orbital (MO) theory. A systematic conformational analysis for the structures was done at the HF/6-31G* level. The conformers were re-optimized at the HF/6-31G** level. Backbones are rendered in balls-and-cylinders, hydrogen atoms in sticks. Optimization was performed by conjugate gradient algorithm, convergence at 0.001; energies are expressed in Kcal $mol^{-1}$. $DIPEAH^+$ was included in the computations, but is not visualized for clarity.

**Table S7**. Angles ϕ and ψ of the residues *i+1*, *i+2* observed for the compounds analyzed and ideal values.

| compd | $\phi_{i+1}$ | $\psi_{i+1}$ | $\chi_{i+1}$ | $\phi_{i+2}$ | $\psi_{i+2}$ | $\chi_{i+2}$ |
|---|---|---|---|---|---|---|
| **2a** (A) | -73 | 158 | -114 | -81 | 76 | -115 |
| **2a** (B) | -104 | -179 | -90 | -40 | -50 | -140 |
| **2c** (C) | -45 | 129 | -122 | 69 | -86 | 118 |
| **2c** (D) | -51 | 144 | -117 | 77 | -27 | 110 |
| **2d** | -55 | 139 | -117 | 77 | -29 | 113 |
| **3b** | -38 | -59 | -2 | -96 | 29 | -114 |
| **3c** (E) | 61 | 55 | 2 | 93 | -2 | 117 |
| **3c** (F) | 37 | 63 | 0 | 81 | -36 | 113 |
| I | -60 | -30 | - | -90 | 0 | - |
| II | -60 | 120 | - | 80 | 0 | - |

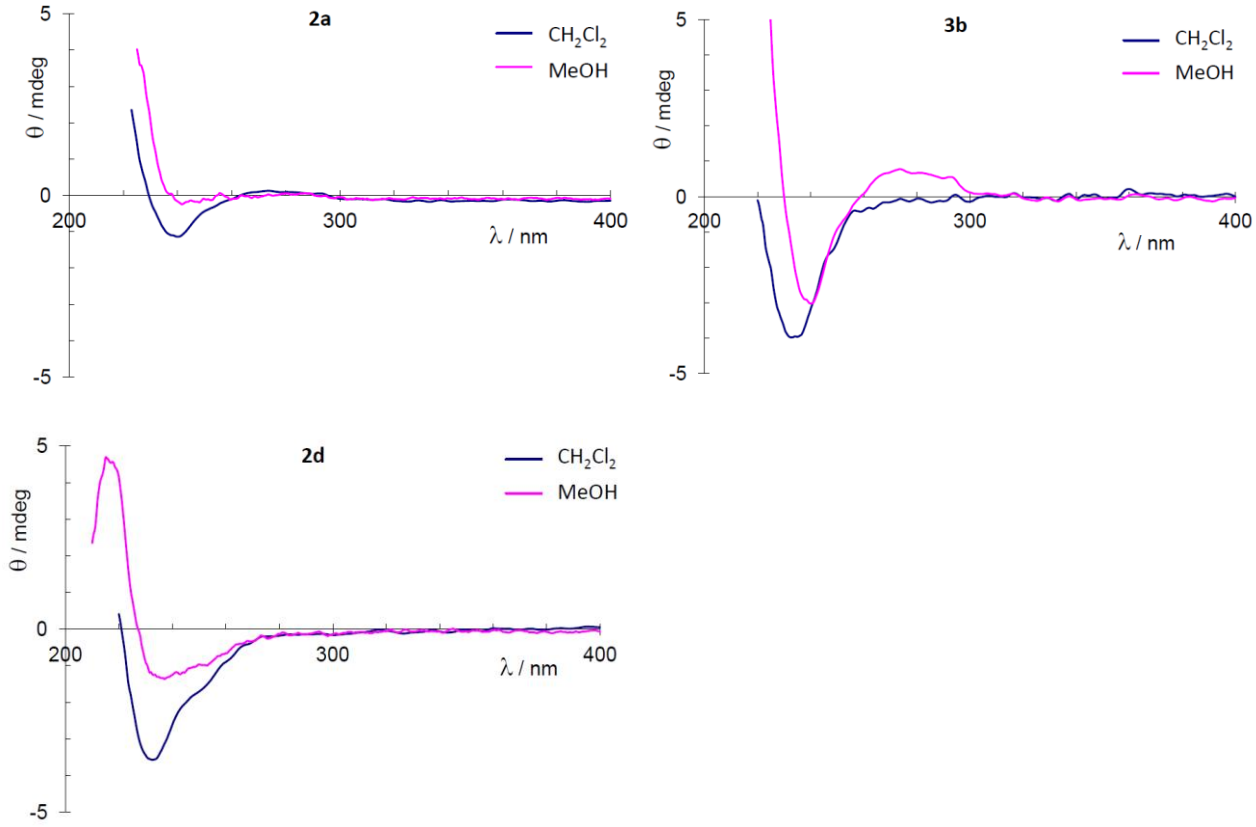


Figure S4. ECD spectra of **2a**, **3b**, and **2d**; 1 mM in DCM or MeOH, path length 0.1 cm.

Figure S5.

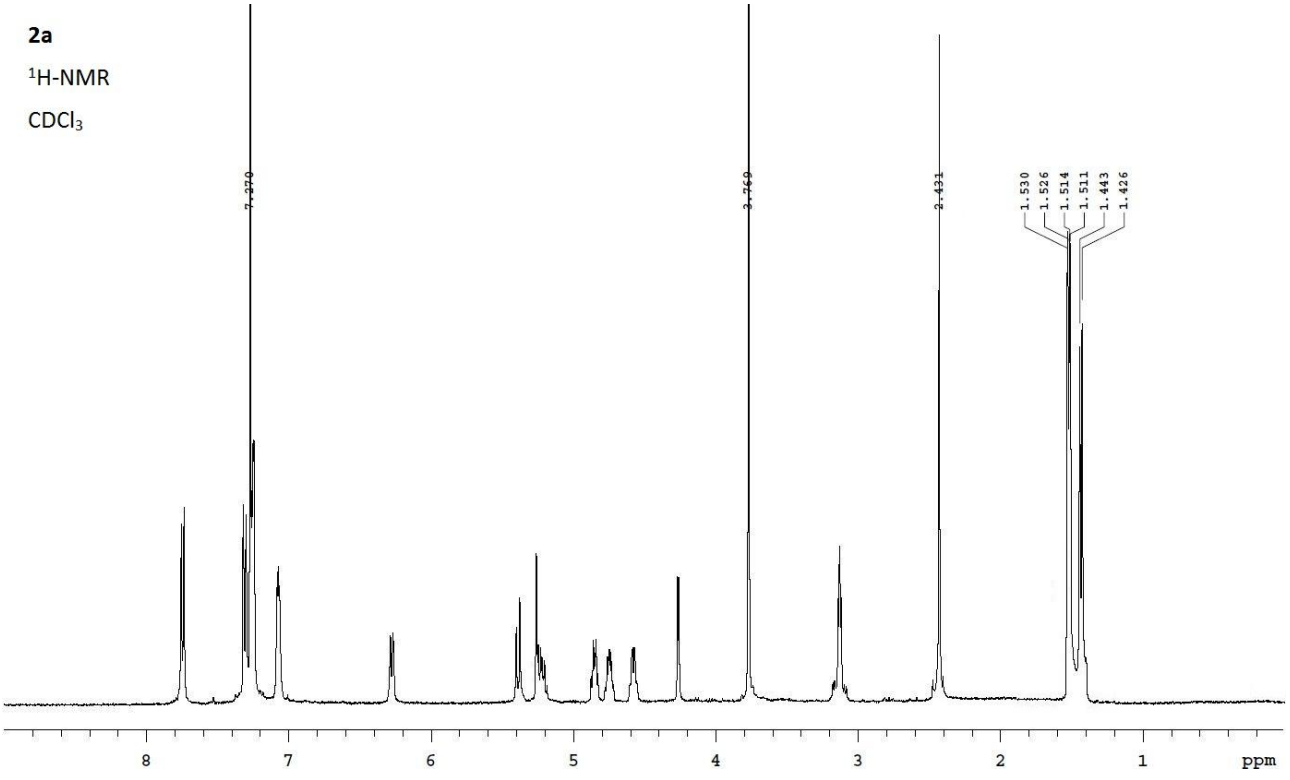
2a
1H-NMR
CDCl3
7.370
3.769
2.431
1.530
1.526
1.514
1.511
1.443
1.426
8
7
6
5
4
3
2
1
ppm

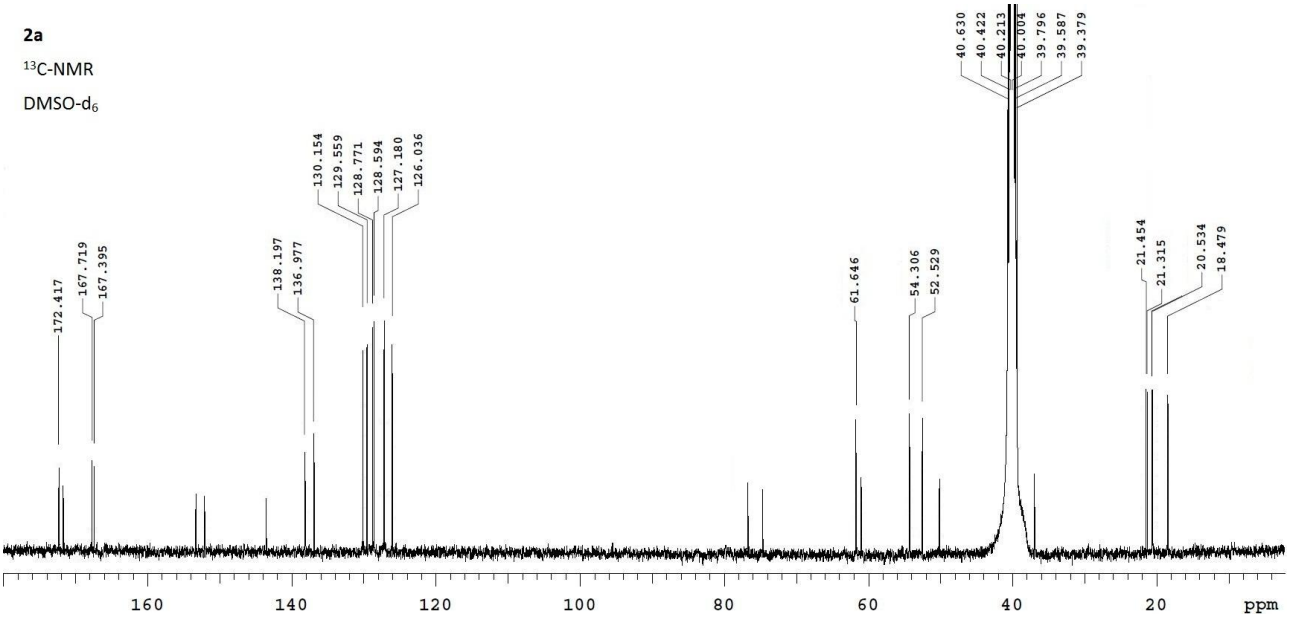
2a
13C-NMR
DMSO-d6
172.417
167.719
167.395
138.197
136.977
130.154
129.559
128.771
128.594
127.180
126.036
61.646
54.306
52.529
40.630
40.422
40.213
40.004
39.796
39.587
39.379
21.454
21.315
20.534
18.479
160
140
120
100
80
60
40
20
ppm

Figure S6.

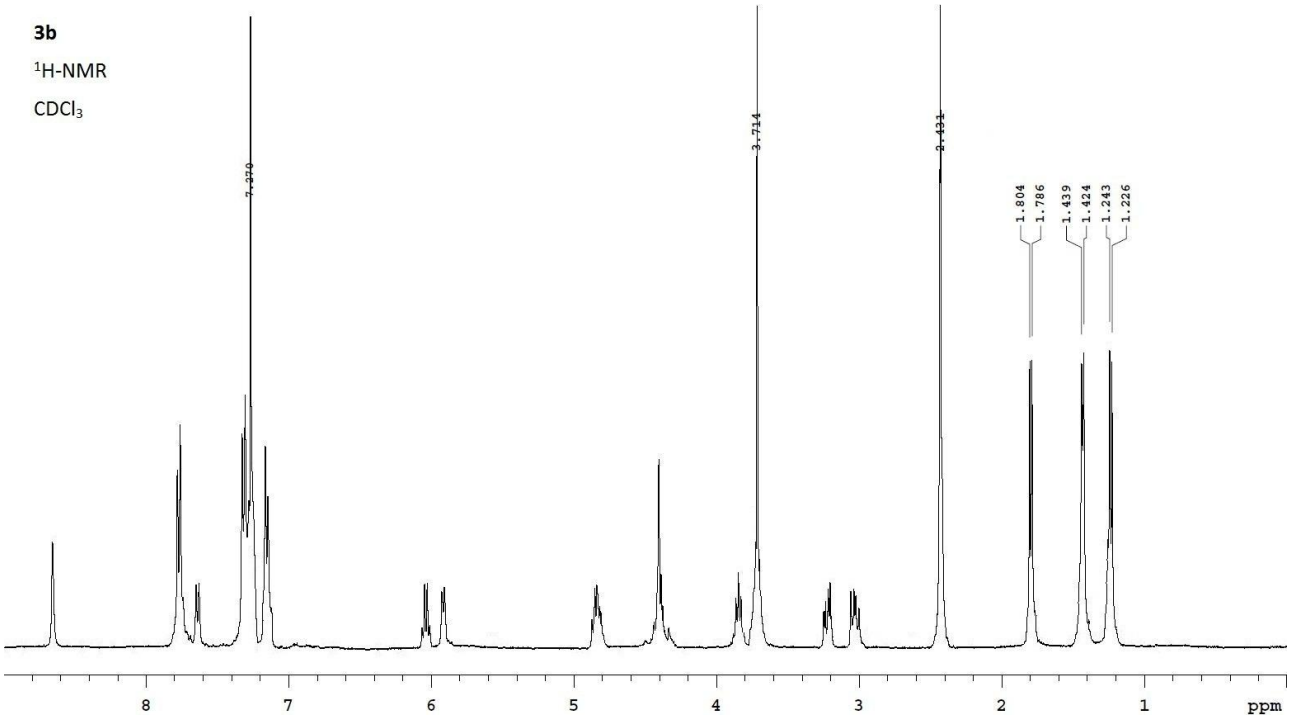
3b
1H-NMR
CDCl3
7.270
3.714
2.431
1.804
1.786
1.439
1.424
1.243
1.226
8
7
6
5
4
3
2
1
ppm

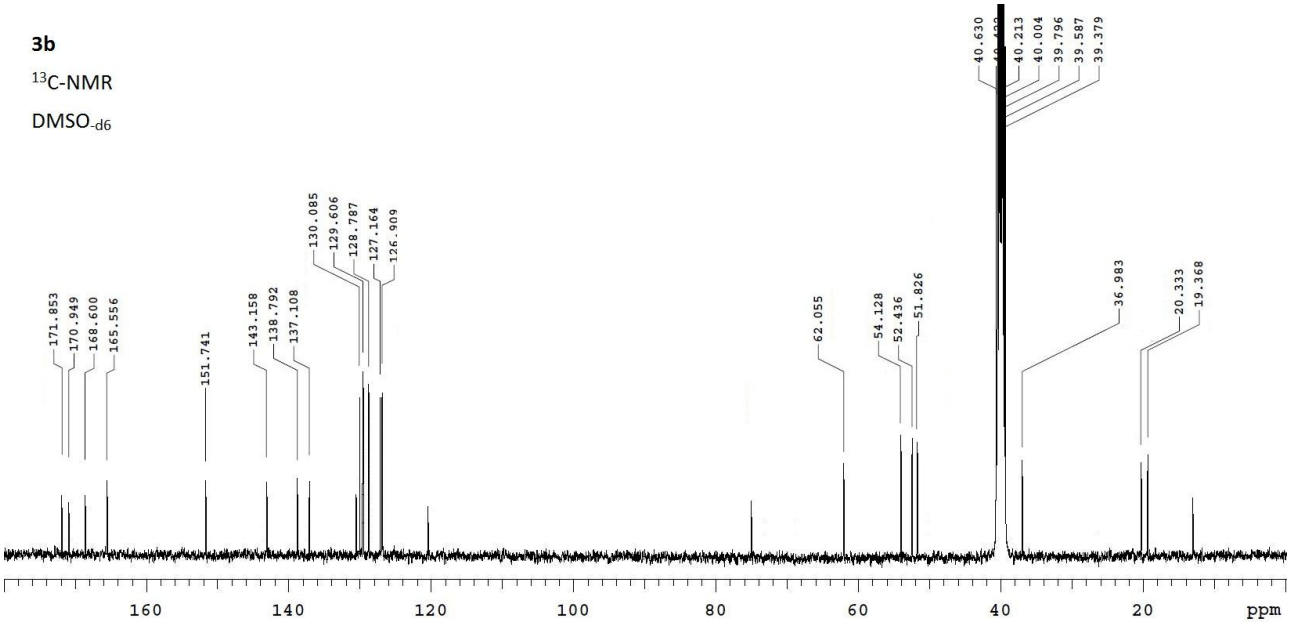
3b
13C-NMR
DMSO-d6
171.853
170.949
168.600
165.556
151.741
143.158
138.792
137.108
130.085
129.606
128.787
127.164
126.909
62.055
54.128
52.436
51.826
40.630
40.213
40.004
39.796
39.587
39.379
36.983
20.333
19.368
160
140
120
100
80
60
40
20
ppm

Figure S7.

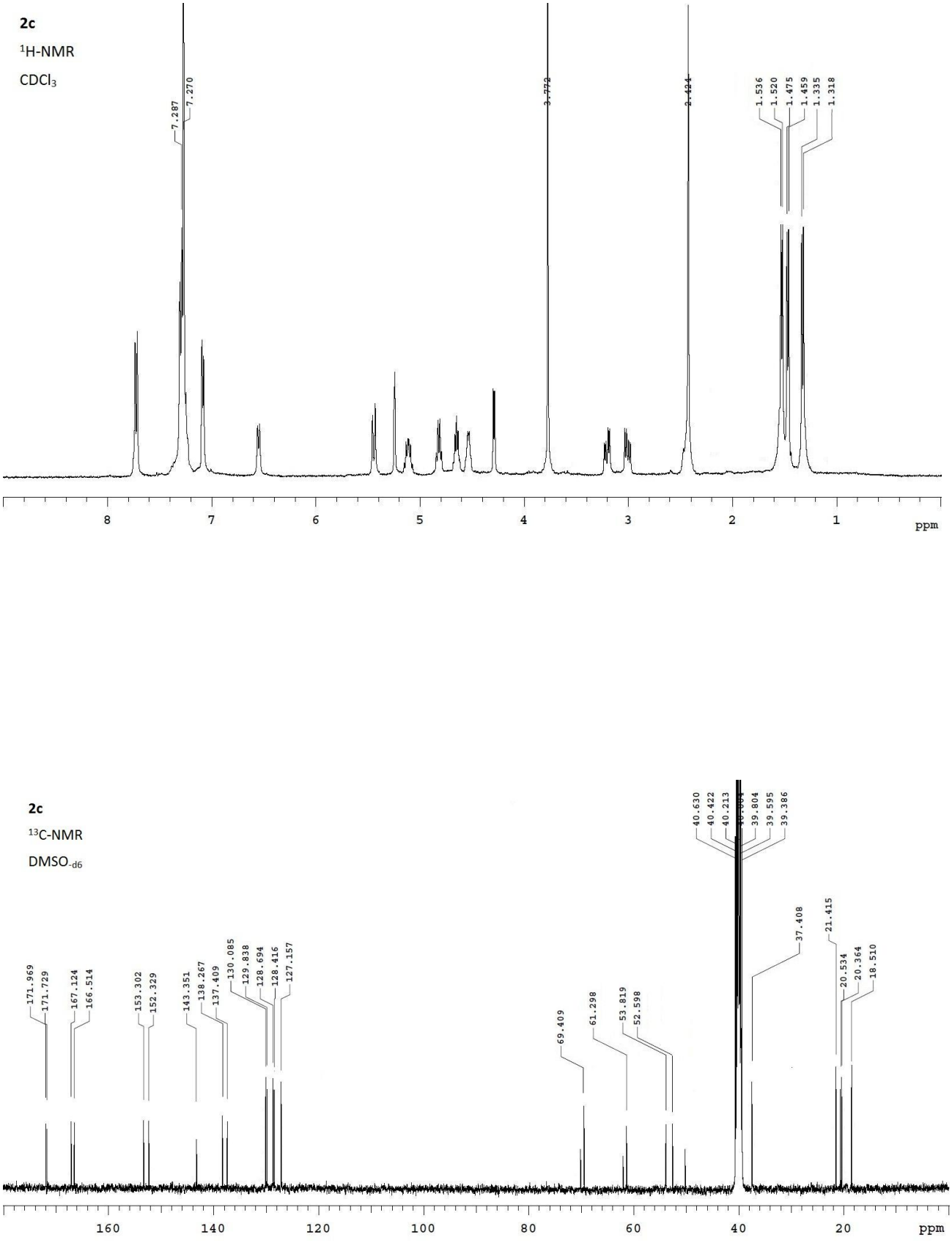

Figure S8.

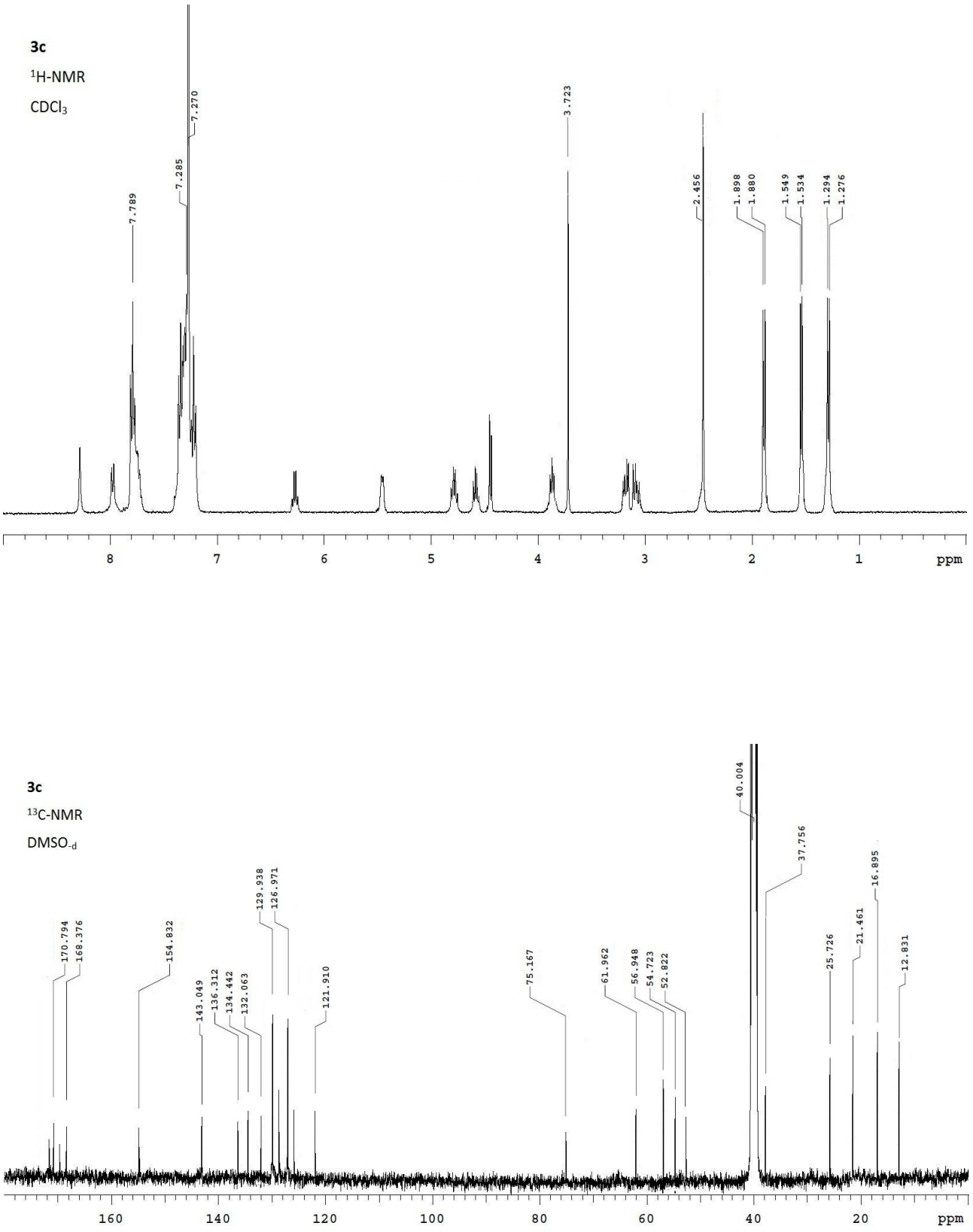
3c
1H-NMR
CDCl3
7.789
7.285
7.270
3.723
2.456
1.898
1.880
1.549
1.534
1.294
1.276
8
7
6
5
4
3
2
1
ppm
3c
13C-NMR
DMSO-d
170.794
168.376
154.832
143.049
136.312
134.442
132.063
129.938
126.971
121.910
75.167
61.962
56.948
54.723
52.822
40.004
37.756
25.726
21.461
16.895
12.831
160
140
120
100
80
60
40
20
ppm

Figure S9.

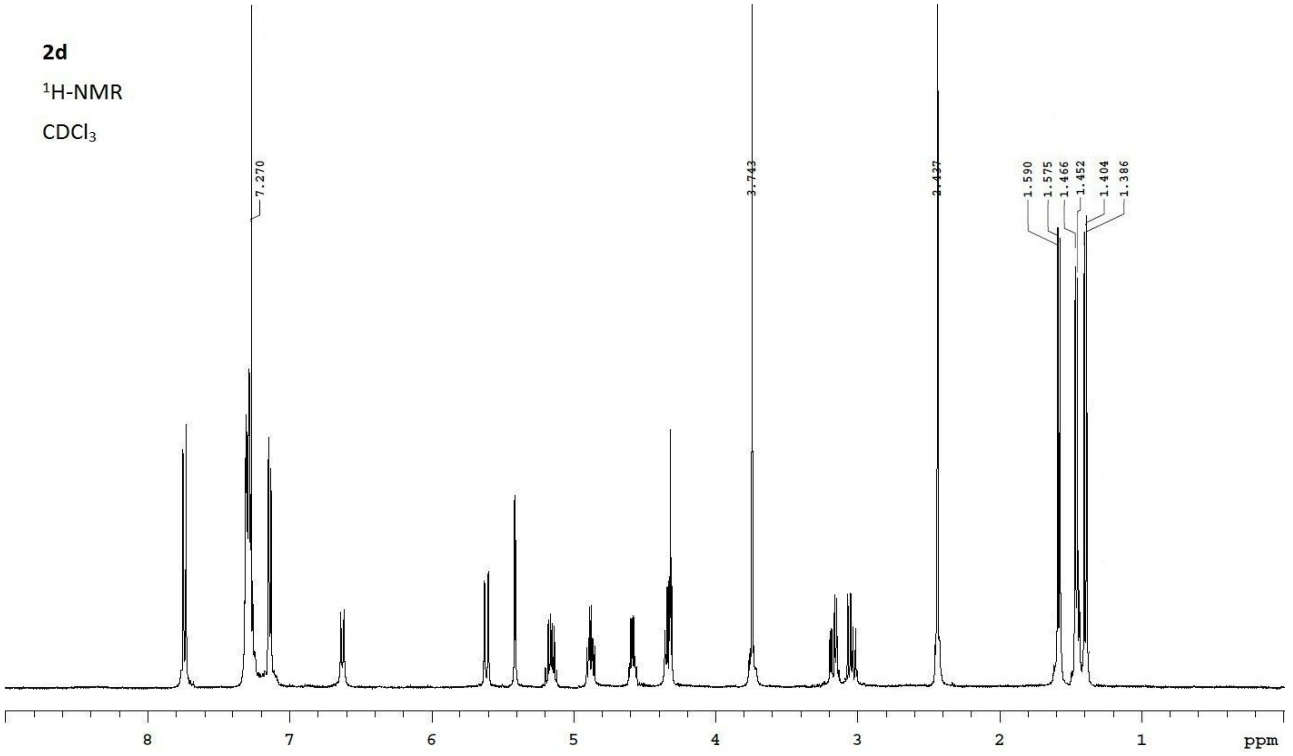
2d
1H-NMR
CDCl3
7.270
3.743
3.437
1.590
1.575
1.466
1.452
1.404
1.386
8
7
6
5
4
3
2
1
ppm

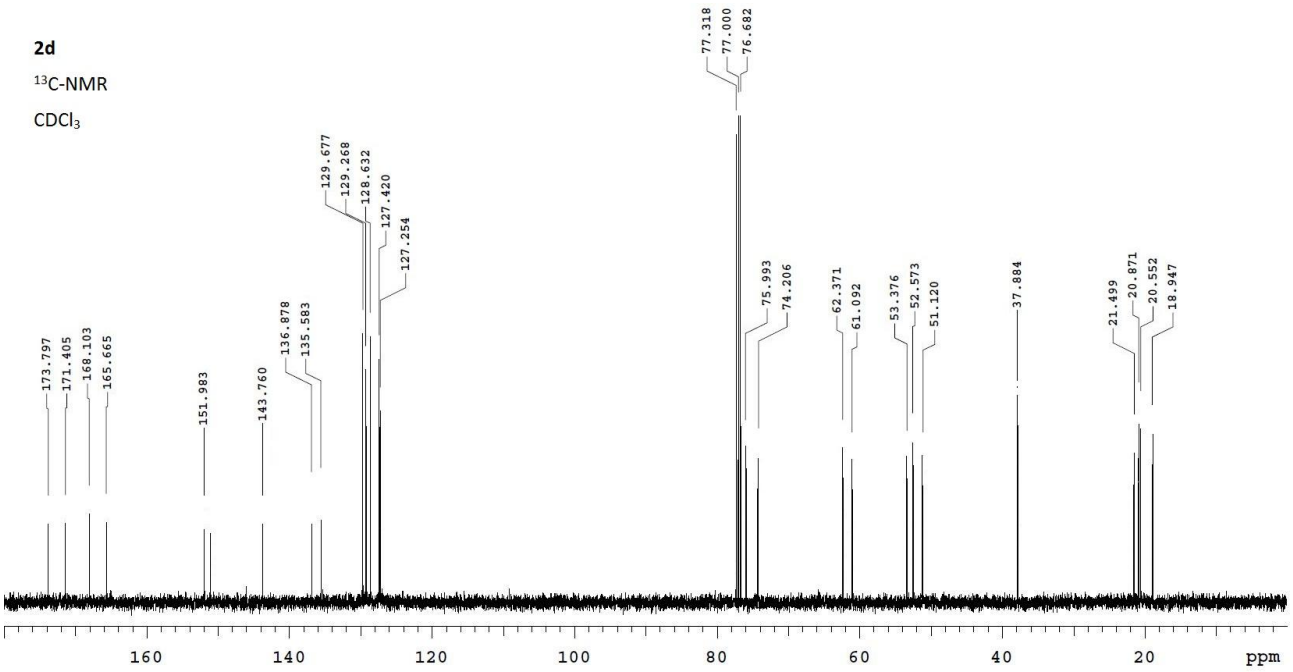
2d
13C-NMR
CDCl3
77.318
77.000
76.682
129.677
129.268
128.632
127.420
127.254
173.797
171.405
168.103
165.665
151.983
143.760
136.878
135.583
75.993
74.206
62.371
61.092
53.376
52.573
51.120
37.884
21.499
20.871
20.552
18.947
160
140
120
100
80
60
40
20
ppm

Figure S10.

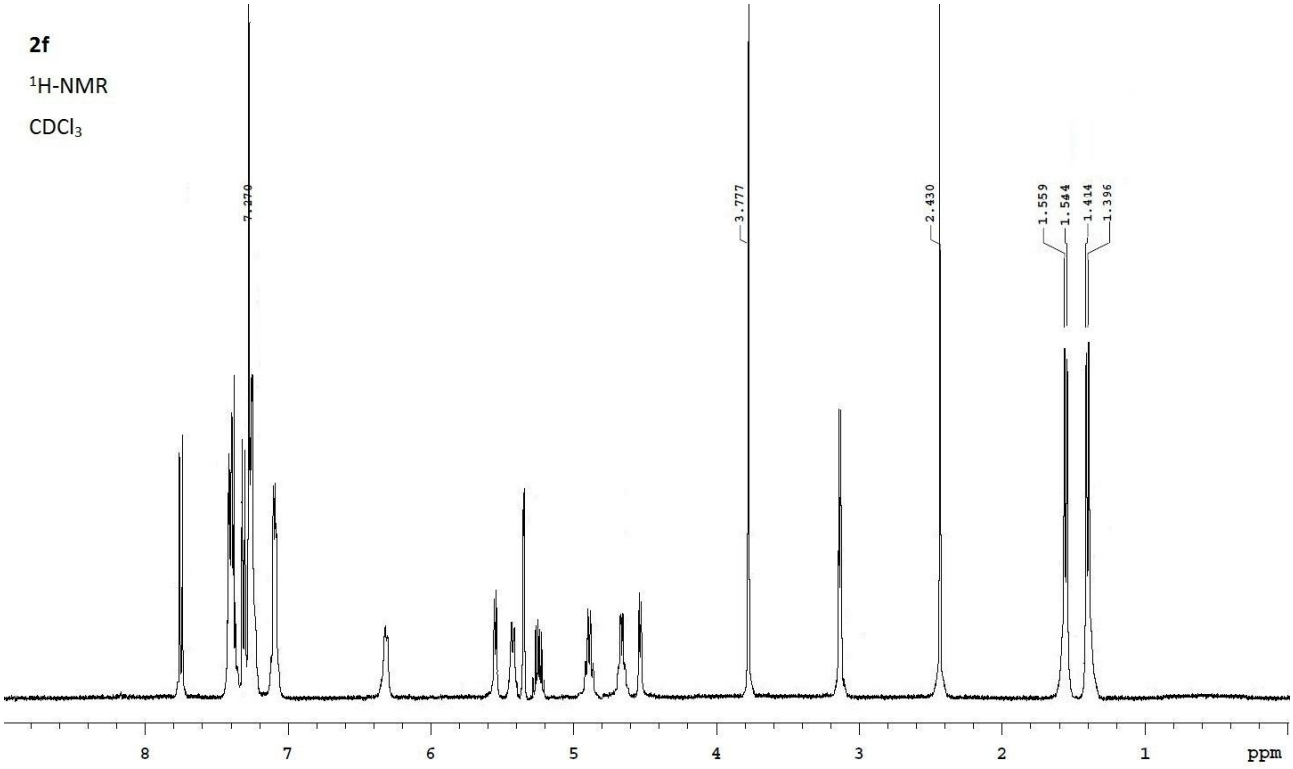
2f
1H-NMR
CDCl3
7.370
3.777
2.430
1.559
1.544
1.414
1.396
8
7
6
5
4
3
2
1
ppm

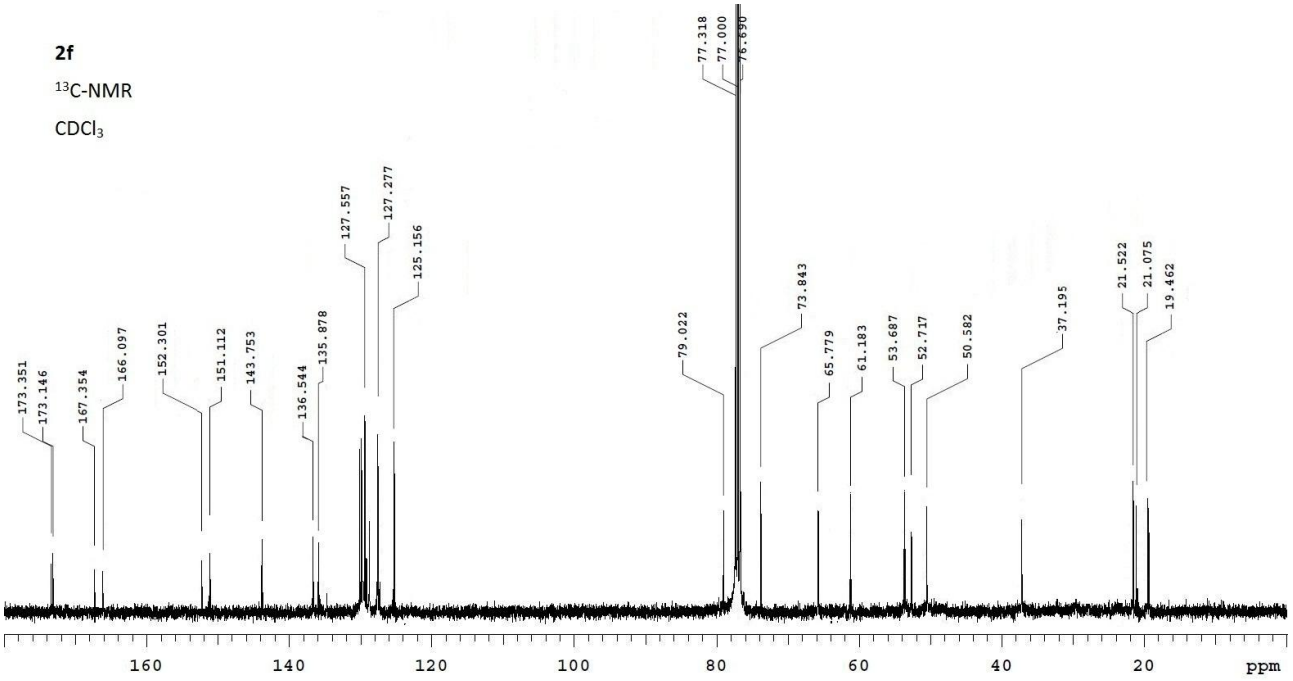
2f
13C-NMR
CDCl3
173.351
173.146
167.354
166.097
152.301
151.112
143.753
136.544
135.878
127.557
127.277
125.156
77.318
77.000
76.690
79.022
73.843
65.779
61.183
53.687
52.737
50.582
37.195
21.522
21.075
19.462
160
140
120
100
80
60
40
20
ppm

Figure S11.

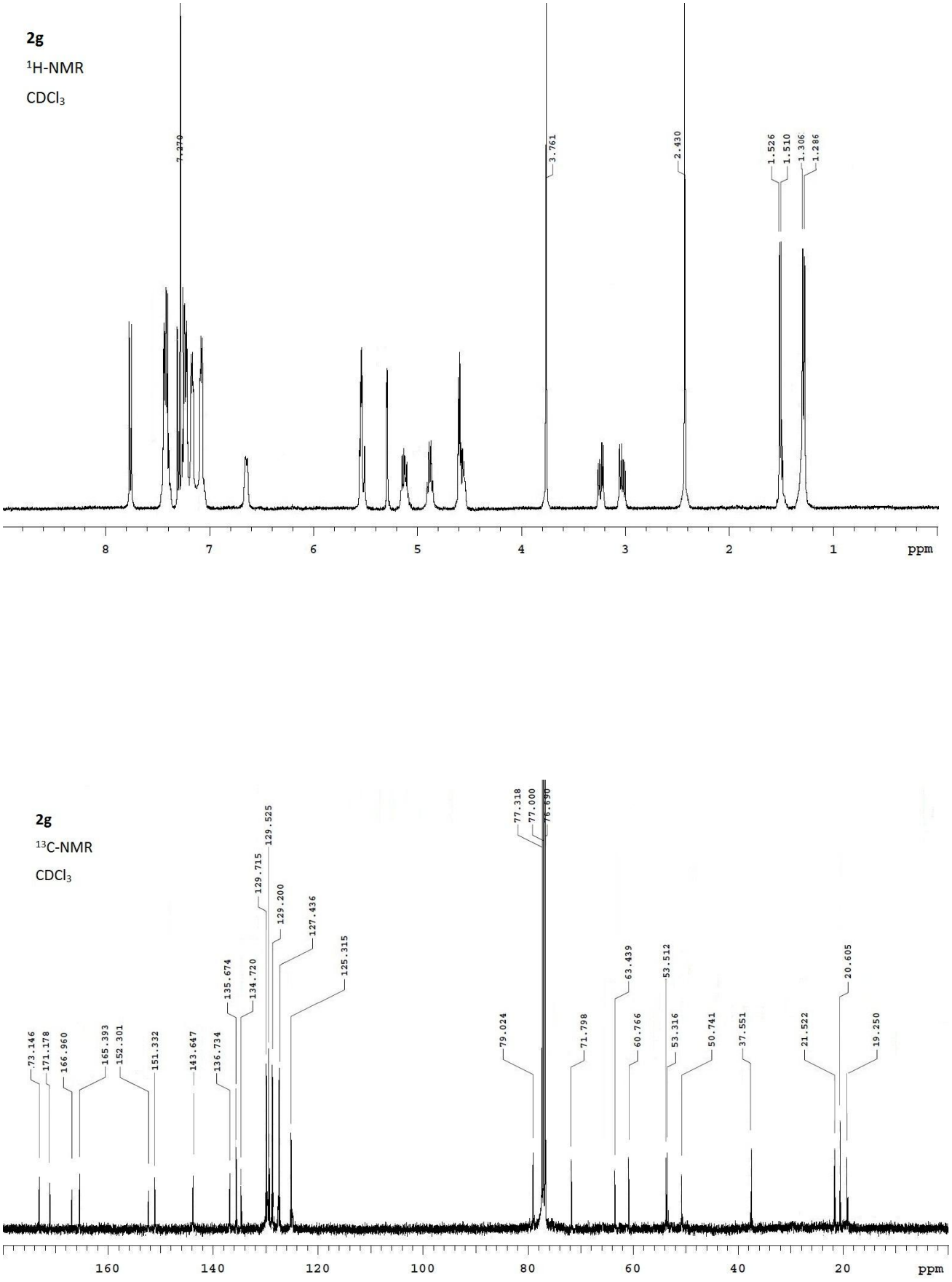
2g
1H-NMR
CDCl3
7.270
3.761
2.430
1.526
1.510
1.306
1.286
8
7
6
5
4
3
2
1
ppm
2g
13C-NMR
CDCl3
77.318
77.000
76.690
129.525
129.715
129.200
127.436
125.315
135.674
134.720
73.146
171.178
166.960
165.393
152.301
151.332
143.647
136.734
79.024
71.798
63.439
60.766
53.512
53.316
50.741
37.551
21.522
20.605
19.250
160
140
120
100
80
60
40
20
ppm